Ligand-to-Ligand Charge-Transfer Photochemistry

Yingsheng Wang, Brian T. Hauser, Michael M. Rooney, Richard D. Burton, and Kirk S. Schanze*

Contribution from the Department of Chemistry, University of Florida, Gainesville, Florida 32611

Received October 26, 1992

Abstract: The photochemistry and photophysics are reported for a unique series of complexes of the type *fac*-(bpy)-$Re^{I}(CO)_3$–(α-AA), where bpy = 2,2′-bipyridine and α-AA is a "reactive donor ligand" that incorporates an α-amino alcohol functionality. Photoexcitation of these complexes into the $d\pi(Re) \rightarrow \pi^*(bpy)$ metal-to-ligand charge-transfer manifold is followed by intramolecular donor ligand (α-AA)-to-metal electron transfer to produce the ligand-to-ligand charge-transfer (LLCT) state $(bpy^{\bullet-})Re^{I}(CO)_3$–$(\alpha\text{-}AA^{\bullet+})$. The reactive donor ligand complexes are designed so that formation of the radical cation (α-$AA^{\bullet+}$) in the LLCT state triggers a rapid C-C bond fragmentation reaction within the α-AA ligand. This photochemical reaction is used to (1) confirm that the LLCT state is formed; (2) explore the kinetic parameters for formation and decay of the LLCT state; (3) to "clock" the rates for the photoinduced intraligand bond-fragmentation process.

Introduction

The photophysics of d^6 transition-metal complexes that contain electron acceptor (A) and electron donor (D) ligands has been the topic of a number of recent investigations. In A–$M(d^6)$–D complexes, the lowest excited state is often based on an electronic configuration which involves ligand-to-ligand charge transfer (LLCT) from the donor to the acceptor ligand, e.g., $A^{\bullet-}$–$M(d^6)$–$D^{\bullet+}$.[1-11] In many A–$M(d^6)$–D complexes, although the LLCT state is the lowest energy configuration, due to poor electronic coupling between the donor and acceptor ligands, radiative transitions between the ground state and the LLCT state have low probability (e.g., the extinction coefficient ϵ and radiative decay rate k_r are small). As a result, the LLCT state is formed indirectly via initial metal-to-ligand charge-transfer (MLCT) excitation followed by rapid donor ligand-to-metal forward electron transfer (ET), and LLCT decay occurs primarily via nonradiative back-ET (see Scheme I). Since the LLCT state is often nonluminescent, its involvement in the photophysics of a complex must be inferred either indirectly from its effect on the properties of the MLCT state or, in favorable cases, from transient absorption studies.[1,2,4,5,8]

Because of the difficulty of studying the kinetics and reactivity of the LLCT state, a new approach has been developed which is based on using "reactive donor ligands" (D–R) which undergo rapid bond-fragmentation upon single electron oxidation. In complexes which feature reactive donor ligands, A–$M(d^6)$–(D–R), the formation and dynamics of the LLCT state can, in principle, be deduced by examining the efficiency for formation of products which result from bond-fragmentation in the LLCT state. A kinetic diagram which highlights the events that occur upon photoexcitation of a D–R-substituted complex is shown in Scheme II.

Scheme I

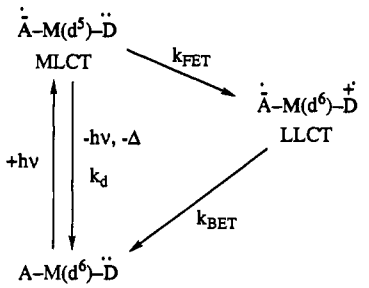

Scheme II

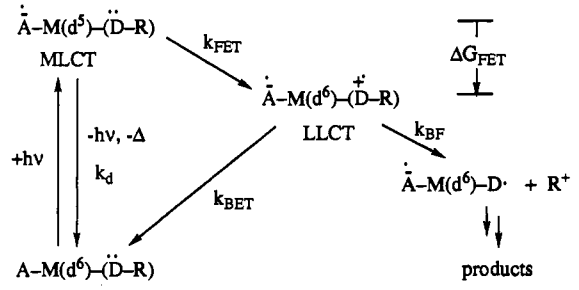

While the concept of using reactive donor (or acceptor) ligands to probe the electronic structure and dynamics of LLCT states in metal complexes is new, this approach has been widely applied to study the structure and dynamics of exciplexes, ion pairs, and free-radical ions formed by photoinduced electron transfer (PET).[12] Examples of reactive donors which have been used as probes in PET reactions include: α-amino alcohols, organoborates, pinacols, bicumenes, strained hydrocarbons, silyl amines, and organometallic ions.[13-25] Although there is a wide range of reactive

(1) Chen, P.; Westmoreland, T. D.; Danielson, E.; Schanze, K. S.; Anthon, D.; Neveaux, P. P.; Meyer, T. J. *Inorg. Chem.* **1987**, *26*, 1116.
(2) Danielson, E.; Elliott, C. M.; Merkert, J. W.; Meyer, T. J. *J. Am. Chem. Soc.* **1987**, *109*, 2519.
(3) Meyer, T. J. *Acc. Chem. Res.* **1989**, *22*, 163.
(4) Perkins, T. A.; Pourreau, D. B.; Netzel, T. L.; Schanze, K. S. *J. Phys. Chem.* **1989**, *93*, 4511.
(5) Perkins, T. A.; Humer, W.; Netzel, T. L.; Schanze, K. S. *J. Phys. Chem.* **1990**, *94*, 2229.
(6) Perkins, T. A.; Hauser, B. T.; Eyler, J. R.; Schanze, K. S. *J. Phys. Chem.* **1990**, *94*, 8745.
(7) MacQueen, D. B.; Schanze, K. S. *J. Am. Chem. Soc.* **1991**, *113*, 6108.
(8) MacQueen, D. B.; Schanze, K. S. *J. Am. Chem. Soc.* **1991**, *113*, 7470.
(9) Schanze, K. S.; MacQueen, D. B.; Perkins, T. A.; Cabana, L. A. *Coord. Chem. Rev.* **1993**, *122*, 63.
(10) Koester, V. J. *Chem. Phys. Lett.* **1975**, *32*, 575.
(11) Truesdell, K. A.; Crosby, G. A. *J. Am. Chem. Soc.* **1985**, *107*, 1787.
(12) Photoinduced Electron Transfer; Fox, M. A., Chanon, M. D., Eds.; Elsevier: Amsterdam, 1988; Parts A–D.
(13) (a) Popielarz, R.; Arnold, D. R. *J. Am. Chem. Soc.* **1990**, *112*, 3068. (b) Okamoto, A.; Snow, M. S.; Arnold, D. R. *Tetrahedron* **1986**, *42*, 6175.
(14) (a) Lewis, F. D.; Bedell, A. M.; Dykstra, R. E.; Elbert, J. E.; Gould, I. R.; Farid, S. *J. Am. Chem. Soc.* **1990**, *112*, 8055. (b) Lewis, F. D. In ref 5, part C, p 1.
(15) (a) Ci, X.; Kellet, M. A.; Whitten, D. G. *J. Am. Chem. Soc.* **1991**, *113*, 3893. (b) Ci, X.; Whitten, D. G. In ref 12, Part C, p 553.

0002-7863/93/1515-5675$04.00/0

donors available, thermodynamic and synthetic considerations led us to focus initial studies on A–M(d^6)–(D–R) complexes which incorporate α-amino alcohols (α-AA) as reactive donor ligands. Recent mechanistic studies by Whitten's group have demonstrated that a structurally diverse set of α-AAs undergo rapid heterolytic C–C bond-fragmentation following PET oxidation (eq 1).[15]

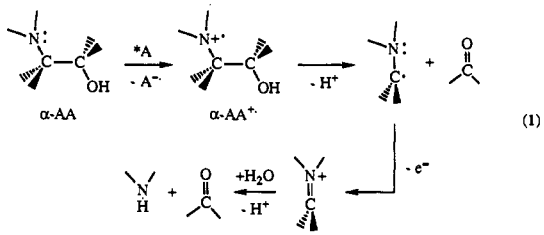

Carbon-carbon bond-fragmentation in α–AA$^{\bullet+}$ produces an α-amino radical and a stable carbonyl compound; further oxidation of the α-amino radical results in formation of an iminium ion which is susceptible to hydrolysis to form a dealkylated amine and a second carbonyl compound.

The present study focuses on the photochemistry and photophysics of two α–AA-based A–M(d^6)–(D–R) complexes **Re-1** and **Re-4**; several additional unreactive donor- and non-donor-substituted complexes (**Re-2**, **Re-3**, **Re-5**, and **Re-6**) have also been examined as models for the photophysics of the (bpy)-Re^I(CO)$_3^-$ chromophore under conditions where formation of the LLCT state and/or bond-fragmentation in the LLCT state are precluded. The (bpy)Re^I(CO)$_3^-$ chromophore was selected for these studies because it has a well-characterized, luminescent MLCT excited state which is based on dπ(Re) → π*(bpy) charge transfer[26-28] and because a variety of recent studies have focused on the photophysics of LLCT states in complexes of the type (bpy)Re^I(CO)$_3$–D, where D is an unreactive electron-donor ligand and bpy is 2,2′-bipyridine.[1-9] The goal of the studies of the reactive donor ligand-substituted complexes is several-fold: (1) to survey the photochemistry of D–R-substituted complexes to establish that reactivity characteristic of (D–R)$^{\bullet+}$ indeed occurs under conditions where the LLCT state is formed; (2) to quantify the kinetic parameters for the D–R complexes and to "clock" the rates for bond-fragmentation in the LLCT state; and (3) to survey several D–R ligands and assess their utility as probes in studies of other A–M(d^6)–(D–R) complexes.

Experimental Section

General Synthetic. Solvents and chemicals used for synthesis were of reagent grade and used without purification unless noted. Silica gel (Merck, 230–400 mesh) and neutral alumina (Fisher, Brockman grade III) were used for chromatography. NMR spectra were run on either GE QE 300-MHz or Varian XL 200-MHz spectrophotometers. The metal complexes (bpy)Re^I(CO)$_3$Cl and [(bpy)Re^I(CO)$_3$(4-benzylpyridine)][PF$_6$] (**Re-6**) were synthesized as previously described.[8,29] All Re(I) complexes were isolated as PF_6^- salts.

erythro-2-[(4-Pyridyl)methylamino]-1,2-diphenylethanol (1). 4-(Aminomethyl)pyridine (4.1 mL, 4.37 g, 40 mmol) and *trans*-stilbene oxide (1.57 g, 8 mmol) were heated at 100 °C under a blanket of argon. The reaction was monitored by TLC (5% MeOH/CHCl$_3$); heating was discontinued after 6.5 h when the high R_f *trans*-stilbene spot had disappeared completely. The crude product was purified by repeated chromatography on silica, using 40% CH$_3$CN/CH$_2$Cl$_2$ as eluant. Pure **1** was obtained as white crystals, yield 600 mg (25%).

Analytical data: TLC (silica, 40% CH$_3$CN/CH$_2$Cl$_2$) R_f = 0.35; ^{1}H NMR (300 MHz, CDCl$_3$) δ 3.51 (d, J = 14.7 Hz, 1H, diastereotopic CH$_2$), 3.69 (d, J = 14.7 Hz, 1H, diastereotopic CH$_2$), 3.87 (d, J = 6.3 Hz, 1H, benzylic), 4.83 (d, J = 6.3 Hz, 1H, benzylic), 7.07 (d, J = 6.0 Hz, 2H, pyridyl), 7.18–7.37 (m, 10H, phenyls), 8.43 (d, J = 6.0 Hz, 2H, pyridyl); ^{13}C NMR (75 MHz, CDCl$_3$) δ 49.8 (adjacent to pyridyl), 68.1 (benzylic), 77.3 (benzylic), 122.8, 126.9, 127.9, 127.9, 128.2, 128.4 (2C), 139.0, 140.6, 149.1, 149.6 (all aromatic); HRMS (methane CI) calcd for C$_{20}$H$_{21}$N$_2$O (M + H) 305.1654, found 305.1739.

4-[(N-Benzylamino)methyl]pyridine (2). 4-(Aminomethyl)pyridine (5 mL, 5.32 g, 49 mmol) was placed into a 50-mL round-bottom flask which was then purged with argon. The flask was heated to 70 °C, and then α-bromotoluene (1 mL, 1.44 g, 8.4 mmol) was added dropwise over 5 min. The resulting mixture was stirred and heated for 2 h. The crude product was purified by repeated chromatography on silica gel using 7% MeOH/CHCl$_3$ as eluant.

Analytical data: TLC (silica, 7% MeOH/CHCl$_3$) R_f = 0.30; ^{1}H NMR (300 MHz, CDCl$_3$) δ 2.05 (br, NH), 3.81 (s, 2H, CH$_2$), 3.83 (s, 2H, CH$_2$), 7.28 (d, 6.0 Hz, 2H, pyridyl), 7.35 (m, 5H, phenyl), 8.57 (d, 6.0 Hz, 2H, pyridyl); ^{13}C NMR (75 MHz, CDCl$_3$) δ 51.8 (adjacent to pyridyl), 53.2 (benzylic), 123.0, 127.2, 128.1, 128.5, 139.8, 149.4, 149.8 (all aromatic); HRMS (70 eV EI) calcd for C$_{13}$H$_{14}$N$_2$ 198.1155, found 198.115.

***erythro*-1,2-Diphenyl-3-(4-pyridyl)-1-propanol (3).** A solution of phenyllithium in cyclohexane (1.44 M, 7 mL, 10 mmol) was added to a solution of 4-picoline (1.0 g, 10 mmol) in 10 mL of ether that was contained in an argon-purged Schlenk bottle. The resulting solution was stirred at room temperature for 1.5 h, and then it was cooled to −70 °C in a dry ice/2-propanol bath. Then *trans*-stilbene oxide (1.5 g, 7.7 mmol) in 15 mL of ether was added to the cold solution. After being stirred for 30 min, the reaction mixture was warmed to 20 °C and then gently refluxed for an additional 30 min. The reaction mixture was poured into 20 mL of 1 M HCl, and then the mixture was made basic by addition of sufficient Na$_2$CO$_3$. The mixture was extracted 3 times with 30-mL portions of ether, the ether layers were combined and dried, and the solvent was evaporated. The crude product was obtained as 3.5 g of a yellow oil which was purified by repeated chromatography on silica using 5% MeOH/CHCl$_3$ as eluant. Pure **3** was obtained as a white, crystalline solid, yield 700 mg (32%).

Analytical data: TLC (silica, 5% MeOH/CH$_2$Cl$_2$) R_f = 0.30; ^{1}H NMR (300 MHz, CDCl$_3$) δ 2.12 (br, 1H, OH), 2.78–2.93 (m, 2H, diastereotopic CH$_2$), 3.18 (m, 1H, benzylic), 4.87 (d, J = 7.5 Hz, 1H, benzylic) 6.79 (d, J = 6.0 Hz, 2H, pyridyl), 7.12 (m, 2H, phenyls), 7.20–7.40 (m, 8H, phenyls), 8.29 (d, J = 6.0 Hz, 2H, pyridyl); ^{13}C NMR (75 MHz, CDCl$_3$) δ 38.0 (adjacent to pyridyl), 55.3 (benzylic), 77.6 (benzylic), 124.3, 126.8, 127.2, 128.0, 128.4, 128.5, 128.9, 139.3, 142.1, 149.1, 149.3 (all aromatic); HRMS (methane CI) calcd for C$_{20}$H$_{20}$NO (M + H) 290.1544, found 290.1544.

erythro-*N*-(1,2-Diphenyl-2-hydroxyethyl)-*p*-[(4-pyridyl)methyl]aniline (4). (a) ***p*-[(4-Pyridyl)methyl]aniline.** *p*-[(4-Pyridyl)methyl]nitrobenzene (6.3 g, 30 mmol) and Fe powder (18.5 g, 33 mmol) were

(16) (a) Gassman, P. G. In ref 12, Part C, p 70. (b) Gassman, P. G.; Yamaguchi, R. *Tetrahedron* **1982**, *38*, 1113.
(17) (a) Sankararaman, S.; Perrier, S.; Kochi, J. K. *J. Am. Chem. Soc.* **1989**, *111*, 6448.
(18) (a) Maslak, P.; Kula, J.; Chateauneuf, J. E. *J. Am. Chem. Soc.* **1991**, *113*, 2304. (b) Maslak, P.; Asel, S. L. *J. Am. Chem. Soc.* **1988**, *110*, 8260. (c) Maslak, P.; Chapman, W. H., Jr. *J. Org. Chem.* **1990**, *55*, 6334.
(19) (a) Dinnocenzo, J. P.; Todd, W. P.; Simpson, T. R.; Gould, I. R. *J. Am. Chem. Soc.* **1990**, *113*, 2462. (b) Dinnocenzo, J. P.; Farid, S.; Goodman, J. L.; Gould, I. R.; Todd, W. P.; Mattes, S. L. *J. Am. Chem. Soc.* **1989**, *111*, 8973.
(20) (a) Lan, J. Y.; Schuster, G. B. *J. Am. Chem. Soc.* **1985**, *107*, 6719. (b) Lan, J. Y.; Schuster, G. B. *J. Am. Chem. Soc.* **1986**, *27*, 4261. (c) Chattergee, S.; Davis, P. D.; Gottschalk, P.; Kurz, M. E.; Saurwein, B.; Yang, X.; Schuster, G. B. *J. Am. Chem. Soc.* **1990**, *112*, 6329.
(21) (a) Eaton, D. F. *J. Am. Chem. Soc.* **1980**, *102*, 3278. (b) Eaton, D. F. *J. Am. Chem. Soc.* **1981**, *103*, 7235.
(22) (a) Jones, G., III; Chiang, S.-H.; Becker, W. G.; Greenberg, D. P. *J. Chem. Soc., Chem. Commun.* **1980**, 681. (b) Jones, G., III; Chiang, S.-H. *Tetrahedron* **1981**, *37*, 3397. (c) Jones, G., III; Becker, W. G. *Chem. Phys. Lett.* **1982**, *85*, 271. (d) Jones, G., III; Chiang, S.-H.; Becker, W. G.; Welch, J. A. *J. Phys. Chem.* **1982**, *86*, 2805. (e) Roth, H. D.; Schilling, M. L. M.; Jones, G., III *J. Am. Chem. Soc.* **1981**, *103*, 1246.
(23) Saeva, F. D.; Breslin, D. T.; Luss, H. R. *J. Am. Chem. Soc.* **1991**, *113*, 5333.
(24) (a) Brumfield, M. A.; Quillen, S. L.; Yoon, U.-C.; Mariano, P. S. *J. Am. Chem. Soc.* **1984**, *106*, 6855. (b) Hasegawa, E.; Xu, W.; Mariano, P. S.; Yoon, U.-C.; Kim, J.-U. *J. Am. Chem. Soc.* **1988**, *110*, 8099. (c) Hasegawa, E.; Brumfield, M. A.; Mariano, P. S. *J. Org. Chem.* **1988**, *53*, 5435. (d) Xu, W.; Jeon, Y. T.; Hasegawa, E.; Yoon, U.-C.; Mariano, P. S. *J. Am. Chem. Soc.* **1989**, *111*, 406.
(25) (a) Sankaraman, S.; Perrier, S.; Kochi, J. K. *J. Am. Chem. Soc.* **1989**, *111*, 6448. (b) Bockman, T. M.; Kochi, J. K. *J. Am. Chem. Soc.* **1989**, *111*, 4669.
(26) Wrighton, M. S.; Morse, D. L. *J. Am. Chem. Soc.* **1974**, *96*, 998.
(27) Giordano, P. J.; Wrighton, M. S. *J. Am. Chem. Soc.* **1979**, *101*, 2888.
(28) Worl, L. A.; Deusing, R.; Chen, P.; Della Ciana, L.; Meyer, T. J. *J. Chem. Soc., Dalton Trans.* **1991**, 849.
(29) MacQueen, D. B.; Schanze, K. S. *J. Am. Chem. Soc.* **1992**, *114*, 1897.

added to a mixture of 24 mL of absolute ethanol, 6 mL of H_2O, and 0.3 mL of concentrated HCl. The mixture was heated at reflux for 2 h under a stream of N_2. The reaction mixture was cooled, the Fe powder was filtered out, and the residue was washed with excess hot ethanol. The combined filtrate was evaporated, leaving 5.1 g of a light tan product. The product was purified by chromatography on silica gel, using 30% CH_3CN/CH_2Cl_2 as eluant.

(b) Compound 4. This compound was prepared by a variation of a literature method for preparation of α-amino alcohols.[30,31] *p*-[(4-pyridyl)-methyl]aniline (370 mg, 2.0 mmol) was dissolved in 15 mL of CH_2Cl_2 in a 100-mL round-bottom flask. The solution was purged with Ar and cooled to 0 °C. A solution of $AlMe_3$ in CH_2Cl_2 (1.4 mL, 2.5 mmol) was then added slowly via a syringe. The resulting mixture was kept cold and stirred for 30 min. At this time a solution of *trans*-stilbene oxide (328 mg, 1.67 mmol) dissolved in 3 mL of CH_2Cl_2 was added via a syringe. The reaction mixture was allowed to come to room temperature and was stirred for 4 h. After this time, 6 mL of a 6 M $NaOH_{(aq)}$ solution was added, and the mixture was stirred for 1 h. An additional 40 mL of CH_2Cl_2 was added, and the organic layer was separated and dried over Na_2SO_4. The CH_2Cl_2 was evaporated, and the crude product was purified by repeated chromatography: (a) silica gel using 35% CH_3CN/CH_2Cl_2 as eluant; (b) alumina using 5% CH_3CN/5% cyclohexane/CH_2Cl_2 as eluant. Pure **4** was obtained as an off-white powder, yield 260 mg (41%).

Analytical data: TLC (silica gel, 35% CH_3CN/CH_2Cl_2 eluant) R_f = 0.35; ^{1}H NMR (300 MHz, $CDCl_3$) δ 3.70 (s, 2H, benzylic CH_2), 4.55 (d, J = 4.8 Hz, 1H, CH), 4.98 (d, 4.8 Hz, 1H, CH), 6.39 (d, J = 8.4 Hz, 2H, aniline), 6.77 (d, J = 8.4 Hz, 2H, aniline), 6.95 (d, J = 5.7 Hz, 2H, pyridyl), 7.00–7.10 (m, 4H, phenyl), 7.13–7.22 (m, 6H, phenyl), 8.30 (d, J = 5.7 Hz, 2H, pyridyl); ^{13}C NMR ($CDCl_3$, 75 MHz) δ 40.2 (benzylic), 63.8 (CH), 77.0 (CH), 114.1, 124.1 (2C), 126.6, 127.4, 127.7, 127.8, 128.0, 128.1, 129.6, 138.7, 140.4, 145.7, 149.3, 151.2 (all aromatic); HRMS (methane CI) calcd for $C_{26}H_{25}N_2O$ (M + H) 381.1967, found 381.2015.

***p*-[(4-Pyridyl)methyl]-*N*,*N*-dimethylaniline (5).** *p*-[(4-Pyridyl)methyl]-aniline (see above for synthesis) (1.5 g, 8.1 mmol), formaldehyde (1.9 mL, 37% aqueous), and formic acid (1.9 g, 97% solution) were combined and heated over a steam bath for 1 h. After this time the reaction was cooled, whereupon 1.4 mL of concentrated HCl was added. The solution was concentrated under vacuum, and the remaining viscous liquid was added to 20 mL of H_2O. The liquid was basified by addition of 25% $NaOH_{(aq)}$, at which point a sticky solid separated. The solid was isolated by extracting the aqueous suspension with several portions of $CHCl_3$. The $CHCl_3$ layer was dried and concentrated under reduced pressure. The crude product was purified by chromatography on silica gel, using 15% CH_3CN/CH_2Cl_2 as eluant. Pure **5** was obtained as a yellow crystalline solid, yield after purification 150 mg (10%).

Analytical data: TLC (silica gel, 15% CH_3CN/CH_2Cl_2) R_f = 0.25; ^{1}H NMR ($CDCl_3$, 300 MHz), δ 2.91 (s, 6H, 2 × CH_3), 3.85 (s, 2H, benzylic), 6.68 (d, J = 8.8 Hz, 2H, aniline), 7.03 (d, J = 8.8 Hz, 2H, aniline), 7.10 (d, J = 6.0 Hz, 2H, pyridyl), 8.48 (d, J = 6.1 Hz, 2H, pyridyl).

General Procedure for Preparation of Re Complexes. In a typical preparation, (bpy)$Re^I(CO)_3Cl$ (0.25 mmol), $AgPF_6$ (0.5 mmol), and the substituted pyridine ligand (**1–6**, 0.5 mmol) were dissolved in 3 mL of DMF. The solution was purged with argon and then heated to 75 °C. The reactions were monitored by TLC (silica gel, 5% MeOH/$CHCl_3$ eluant), and heating was discontinued when the yellow fluorescent spot due to the product was not increasing any longer; typical time required was 2–3 h. After cooling, the solution was filtered through a medium-porosity fritted filter, and the DMF was evaporated under reduced pressure. The products were purified by chromatography on alumina using gradient elution (10% CH_3CN/CH_2Cl_2–50% CH_3CN/CH_2Cl_2). Typical yield after purification was 40–50%.

Re-1. Analytical data: ^{1}H NMR (300 MHz, CD_3CN) δ 3.32 (br, 1H, NH), 3.41 (d, 1H, diastereotopic CH_2), 3.47 (d, 1H, diastereotopic CH_2), 3.62 (d, 1H, benzylic), 4.72 (d, 1H, benzylic), 7.01 (d, 2H, pyridyl), 7.05–7.28 (m, 10H, phenyls), 7.80 (m, 2H, bpy), 8.00 (d, 2H, pyridyl), 8.28 (tt, 2H, bpy), 8.39 (d, 2H, bpy), 9.21 (d, 2H, bpy); ^{13}C NMR (75 MHz, CD_3CN) δ 48.6 (adjacent to pyridyl), 67.7 (benzylic), 76.3 (benzylic), 124.3, 125.1, 126.6, 126.9, 127.0, 127.5 (2C), 128.3, 128.5, 139.8, 140.8, 142.0, 150.8, 153.5, 155.2, 155.4 (all aromatic).

Re-2. Analytical data: ^{1}H NMR (300 MHz, CD_3CN) δ 3.70 (s, 2H, CH_2), 3.80 (s, 2H, CH_2), 7.33 (m, 7H, phenyl and pyridyl), 7.90 (t, 2H, bpy), 8.22 (d, 2H, pyridyl), 8.38 (t, 2H, bpy), 8.49 (d, 2H, bpy), 9.32 (d, 2H, bpy).

Re-3. Analytical data: ^{1}H NMR (300 MHz, CD_3CN) δ 2.83 (m, 2H, diastereotopic CH_2), 3.08 (m, 1H, benzylic), 3.25 (d, 1H, OH), 4.80 (dd, 1H, benzylic), 6.83 (d, 2H, pyridyl), 6.95 (m, 2H, phenyls), 7.05–7.25 (m, 8H, phenyls), 7.75 (m, 2H, bpy), 7.85 (d, 2H, pyridyl), 8.20–8.35 (m, 4H, bpy), 9.15 (dd, 2H, bpy); ^{13}C NMR (75 MHz, CD_3CN) δ 37.5 (adjacent to pyridyl), 53.4 (benzylic), 76.2 (benzylic), 124.2, 126.2, 126.3, 126.8, 127.0, 127.4, 127.6, 128.4, 128.7, 139.6, 140.8, 143.0, 150.5, 153.4, 154.6, 155.2 (all aromatic).

Re-4. Analytical data: ^{1}H NMR (CD_3CN, 300 MHz), δ 4.54 (dd, 1H, CH), 4.96 (br d, 1H, NH), 5.22 (d, 1H, CH), 6.42 (d, 2H, aniline), 6.70 (d, 2H, aniline), 6.99 (d, 2H, pyridyl), 7.15–7.25 (m, 10H, phenyls), 7.74 (t, 2H, bpy), 8.01 (d, 2H, pyridyl), 8.23 (t, 2H, bpy), 8.34 (d, 2H, bpy), 9.15 (d, 2H, bpy); ^{13}C NMR (CD_3CN, 75 MHz), δ 39.0 (benzylic), 62.8 (benzylic), 75.8 (benzylic), 113.3, 117.0, 124.4, 125.6, 126.2, 126.4, 126.6, 126.9, 127.3, 127.4, 128.1, 128.4, 129.2, 139.9, 140.8, 142.0, 146.0, 151.1, 153.4, 155.4, 156.0 (all aromatic).

Re-5. Analytical data: ^{1}H NMR (CD_3CN, 300 MHz), δ 2.81 (s, 6H, 2 × CH_3), 3.76 (s, 2H, benzylic), 6.62 (d, 2H, aniline), 6.92 (d, 2H, aniline), 7.10 (d, 2H, pyridyl), 7.78 (t, 2H, bpy), 8.09 (d, 2H, bpy), 8.27 (t, 2H, bpy), 8.37 (d, 2H, pyridyl), 9.19 (d, 2H, bpy); ^{13}C NMR (CD_3CN, 75 MHz) δ 40.3 (aliphatic), 40.7 (aliphatic), 113.8, 118.3, 125.6, 126.3, 127.4, 129.8, 130.6, 142.1, 152.5, 154.7, 156.7, 157.4 (all aromatic).

Equipment. Steady-state emission spectra were obtained on a Spex Industries F-112A spectrophotometer. Emission spectra were corrected for instrument response with correction factors that were generated using a tungsten filament primary standard lamp. UV–visible spectra were run on a Perkin-Elmer Model 320 spectrophotometer. Emission lifetimes were measured on a Photochemical Research Associates time-correlated single photon counting spectrophotometer. Emission lifetimes were computed using the DECAN deconvolution package which was provided by Prof. F. C. DeSchryver. Preparative scale photolyses were carried out using a 450-W Hanovia medium-pressure Hg arc lamp which was contained in a Pyrex cooling well. The 366-nm Hg line was isolated using Corning 7-54 and Schott LG 350-nm filters. Quantum yield studies were carried out using a 75-W high-perssure Hg lamp housed in an elliptical reflector housing (PTI ALH-1000). The output from the 75-W lamp was passed through a grating monochromator and focused into a small compartment which contained the sample cell. HPLC was carried out on a system that was comprised of a Waters isocratic pump, a Valco injector, an ABI variable wavelength absorption detector, and a Hewlett-Packard integrating recorder. The HPLC column used was either a Du Pont analytical column (Zorbax C_{18}) or a Whatman semipreparative column (ODS-3). HPLC analysis of the metal complexes required a mobile phase consisting of MeOH/THF/H_2O (35:35:30 v:v:v) with 1 mM sodium heptanesulfonate added as an ion-pairing reagent. Analyses of organic products were carried out with MeOH/H_2O (80:20 v:v) mobile phase. Laser flash photolysis experiments were carried out on a system similar to one that has been previously described.[32] Cyclic voltammetry was carried out using a BAS CV-2 voltammograph with Pt disk working and Pt wire auxilliary electrodes and a saturated sodium chloride calomel (SSCE) reference electrode.

Photophysical and Photochemical Studies. Steady-state and time-resolved emission studies were carried out using procedures that have been previously described.[4] Photochemical quantum yields were determined by irradiation of 3-mL aliquots of a solution containing the reactive complex for various time increments using the 75-W high-pressure Hg source (366 nm). Following irradiation of the sample, a benzophenone internal standard was added to each aliquot, and the samples were analyzed by triplicate injections into the HPLC. Quantum yields were determined from the slope of a plot of moles produced (or consumed) vs irradiation time. The light intensity was determined each day by using the Aberchrome 540 actinometer.[33]

Results

Prior to discussing the results obtained with the various Re(I) complexes, it is important to point out the rationale behind the

(30) Overman, L. E.; Flippin, L. A. *Tetrahedron Lett.* **1981**, *22*, 195.

(31) In the method reported in ref 30, $AlEt_3$ was used instead of $AlMe_3$. An interesting finding is that use of $AlEt_3$ in this reaction produced product **4** which was contaminated with approximately 25–30% of the *threo* isomer. By contrast, reaction using $AlMe_3$ produced **4** which did not contain the *threo* isomer at levels which were detectable by NMR (<5%).

(32) Schanze, K. S. Ph.D. Dissertation, University of North Carolina, Chapel Hill, 1983.

(33) Heller, H. G.; Langan, J. R. *J. Chem. Soc., Perkin Trans. 1* **1981**, 341.

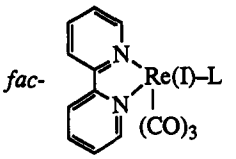

Re-L

Ligands

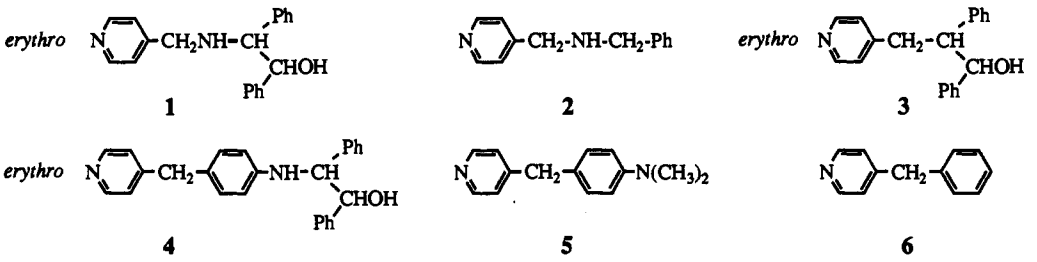

Figure 1. Structures and abbreviations for the metal complex and ligands.

Table I. Electrochemical Potentials[a]

complex	$E(D/D^{\bullet+})$/V	$E_{1/2}(bpy/bpy^{\bullet-})$/V
Re-1	≈1.20 ± 0.2[b]	-1.13
Re-4	+0.94[c]	-1.17
Re-5	+0.82[d]	-1.17
Re-6		-1.16

[a] All potentials in CH_3CN/0.1 M $[(C_4H_9)_4N^+][PF_6^-]$ relative to SSCE reference electrode. [b] E_p value for poorly defined irreversible wave. [c] E_p value for well-defined irreversible wave. [d] $E_{1/2}$ for quasireversible wave ($i_{pc}/i_{pa} \approx 0.25$).

design of each of the structures shown in Figure 1. Complexes **Re-1** and **Re-4** contain the reactive donor α-amino alcohol ligand. These complexes are expected to form and subsequently undergo photochemistry from the LLCT state. Complexes **Re-3** and **Re-6** serve as non-donor-substituted models for complexes **Re-1** and **Re-4**, respectively. Since these complexes do not have an amine donor, they cannot form the LLCT state; they are examined to allow characterization of the MLCT state. Complexes **Re-2** and **Re-5** serve as "nonreactive" donor substituted models for **Re-1** and **Re-4**, respectively. These complexes contain similar aliphatic or aromatic amine donors compared to complexes **Re-1** and **Re-4** and therefore should form the LLCT state with similar rates compared to their reactive counterparts; however, they are not expected to be photochemically reactive.

(a) Electrochemistry. Cyclic voltammetry was carried out on several of the complexes to (1) allow estimation of the free energy for forward ET (ΔG_{FET}) and (2) examine the reversibility of the anodic waves for the D–R ligands. Relevant potentials for complexes **Re-1**, **Re-4**, **Re-5**, and **Re-6** are listed in Table I. All of the complexes display a characteristic, reversible cathodic wave at $E_{1/2} \approx -1.17$ V which is due to reduction of the coordinated bpy acceptor ligand.[9] In addition, each donor-substituted complex displays an anodic wave with a potential and degree of reversibility that depends upon the structure of the ligand (see Figure 2). Complex **Re-5**, in which the donor is an *N,N*-dimethylaniline (DMA) unit, displays a quasireversible wave, which is consistent with the moderate chemical stability of the cation-radical $DMA^{\bullet+}$. By contrast, the anodic wave for **Re-1** and **Re-4** is irreversible, which suggests that in each case the amine radical cation formed by electrochemical oxidation is chemically unstable. Presumably the irreversibility of the anodic process is due to rapid C–C bond-fragmentation which occurs after anodic oxidation. Also, note that the anodic wave for **Re-1** is qualitatively less well-defined than that for **Re-4**; this may signal that the chemical step (bond-fragmentation) that follows electrooxidation is kinetically faster in the former complex.

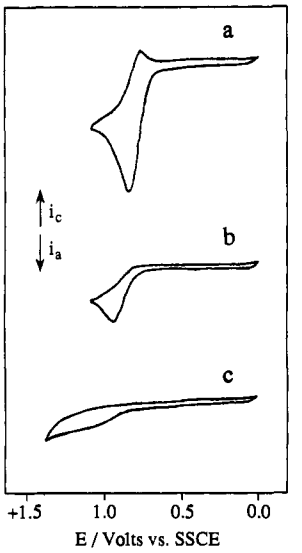

Figure 2. Oxidative cyclic voltammographs for several donor-substituted (bpy)$Re(CO)_3$-L complexes. Sweeps were obtained on 2 mM solutions in CH_3CN/0.1 M tetrabutylammonium hexafluorophosphate with a Pt disk working electrode, SSCE reference, at a sweep rate of 100 mV/s. (a) **Re-5**; (b) **Re-4**; (c) **Re-1**.

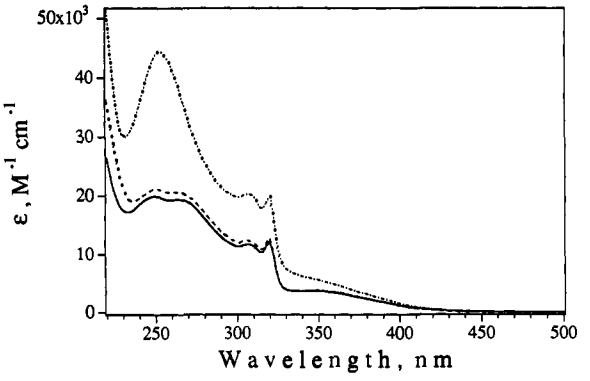

Figure 3. UV–visible absorption spectra of several (bpy)$Re(CO)_3$–L complexes in CH_3CN solution. (—) **Re-6**; (- - -) **Re-1**; (·····) **Re-4**.

(b) Photophysics. Figure 3 shows a comparison of the UV–visible absorption spectra of **Re-1**, **Re-4**, and **Re-6**. Each complex displays a moderately intense absorption in the near-UV region ($\lambda \approx 355$ nm, $\epsilon \approx 4000$ M^{-1} cm^{-1}) which is assigned to the lowest $d\pi(Re) \rightarrow \pi^*(bpy)$ MLCT transition.[9] The intensity of the MLCT absorption is identical for **Re-1** and **Re-6**, indicating that

Table II. Photophysical Data[a]

complex	λ_{em}^{max}/nm ($E_{0,0}$/cm^{-1})[b]	Φ_{em}[c]	τ_{em}/ns[d]	τ_{LLCT}/ns[e]
Re-1	593 (19 200)	0.042	201 ± 3	*f*
Re-2	595 (19 200)	0.041	207 ± 4	*f*
Re-3	593 (19 200)	0.045	212 ± 3	*g*
Re-4	*h*	<0.001	0.5 ± 0.2	12
Re-5	*h*	<0.001		15
Re-6	595 (19 200)	0.045	209 ± 2	*g*

[a] All experiments in Ar-degassed CH_3CN solution with λ_{ex} = 350 nm. [b] Estimated error ±2 nm. $E_{0,0}$ values estimated from Franck–Condon vibronic analysis of emission spectra. [c] Estimated error ±10%. [d] Reported emission lifetimes are average of ≥5 independent measurements; errors are standard deviation in average. [e] Lifetime of the LLCT state determined by laser flash photolysis. [f] Φ_{LLCT} too low to allow determination. [g] Not applicable. [h] Emission too weak for accurate determination.

there is negligible intraligand (π,π^*) absorption in the 360–400-nm wavelength range for these complexes. Complex **Re-4** exhibits slightly stronger absorption in the MLCT region (the near UV) and substantially stronger absorption in the far-UV range compared to **Re-1** and **Re-6**. Examination of the absorption spectrum of α-AA ligand **4** reveals that the increased UV absorptivity of **Re-4** is due to π,π^* (CT) absorption of the α-AA ligand.

Steady-state and time-resolved emission studies were carried out on each of the Re complexes; a summary of the emission data is presented in Table II. Excitation of **Re-1**, **Re-2**, **Re-3**, and **Re-6** at 350 nm produces a moderately intense emission at $\lambda_{max} \approx 595$ nm. This emission is clearly due to the $d\pi(Re) \rightarrow \pi^*(bpy)$ MLCT excited state.[9] The MLCT emission of each complex was characterized by determining the quantum yield and lifetime (Φ_{em} and τ_{em}, respectively). The non-donor-substituted complexes **Re-3** and **Re-6** exhibit remarkably similar Φ_{em} and τ_{em} values, which indicates that the natural decay rate for the MLCT excited state (k_d, Schemes I and II) is not sensitive to the composition of the organic group which is attached to the pyridyl ligand, as long as this group does not contain an electron donor. The Φ_{em} and τ_{em} values for secondary aliphatic amine donor-substituted complexes **Re-1** and **Re-2** are very slightly, but reproducibly, depressed compared to non-donor-substituted complexes **Re-3** and **Re-6**. The slight depression in Φ_{em} and τ_{em} suggests that an additional, nonradiative decay path is operative in **Re-1** and **Re-2**; this pathway is believed to be forward ET to form the LLCT state (k_{FET} path, Schemes I and II).

By contrast, MLCT emission from aromatic amine donor-substituted complexes **Re-4** and **Re-5** is almost completely quenched. Virtually no steady-state emission is observed upon excitation of these complexes at 350 nm; however, a short-lived emission is detected from **Re-4** by using time-correlated single photon counting. The MLCT emission is strongly quenched in these complexes because forward ET is much faster than normal decay of the MLCT state ($k_{FET} \gg k_d$, Schemes I and II). That k_{FET} is faster in complexes **Re-4** and **Re-5** than in **Re-1** and **Re-2** is consistent with the fact that the free energy for this process (ΔG_{FET}) is more exothermic for the aromatic amine donors (*vide infra*).

Laser flash photolysis experiments were conducted on **Re-4**, **Re-5**, and **Re-6** in order to gain spectroscopic and kinetic information on the MLCT and LLCT excited states. Transient spectra of the complexes obtained at various delay times following 355-nm laser excitation (6-ns fwhm, 10 mJ/pulse) are shown in Figure 4. Figure 4a shows the spectrum of **Re-6** obtained at 20-ns delay after excitation. This spectrum is characteristic of the MLCT excited state in $(bpy)Re(CO)_3$–L complexes; the strong band at 370 nm is likely due to a π^*,π^* transition of the bpy anion radical which is present in the MLCT state, e.g., $*[(bpy^{\bullet-})Re^{II}(CO)_3$–L].[5,8,34] Figure 4b shows the transient absorption spectrum of **Re-5** at 0-ns delay after 355-nm excitation. This spectrum differs significantly from that which is typical for the MLCT state; in particular, there is a strong absorption in the mid-visible ($\lambda_{max} \approx 480$ nm) in addition to moderate absorption in the near-UV region. This spectrum is attributed to the LLCT state, $*[(bpy^{\bullet-})Re^{I}(CO)_3$–$DMA^{\bullet+})]$ which is formed from the MLCT state by rapid forward ET following photoexcitation. The LLCT assignment is supported by the presence of the 480-nm absorption band, which coincides with the reported absorption of the *N*,*N*-dimethylaniline radical cation ($DMA^{\bullet+}$).[35] The transient absorption which is assigned to the LLCT state for complex **Re-5** decays with a lifetime of 15 ns. Figure 4c shows the transient absorption spectrum of reactive donor-substituted complex **Re-4** obtained at 0-ns delay after 355-nm excitation. This spectrum is quite similar to the spectrum observed for DMA-substituted complex **Re-5**; in particular, a strong mid-visible absorption band is clearly apparent which can be assigned to the *N*-alkylanilinium radical cation. The mid-visible band in the spectrum of **Re-4** exhibits two maxima (450 and 490 nm), which is interesting in view of the fact that the published absorption spectrum of the *N*-methylanilinium radical cation is dominated by a mid-visible band with two maxima.[35] These facts strongly support the assignment of the transient formed by nanosecond flash photolysis of **Re-4** to the LLCT state. Analysis of the transient absorption decay shows that the LLCT state in reactive donor complex **Re-4** has a lifetime of 12 ns.

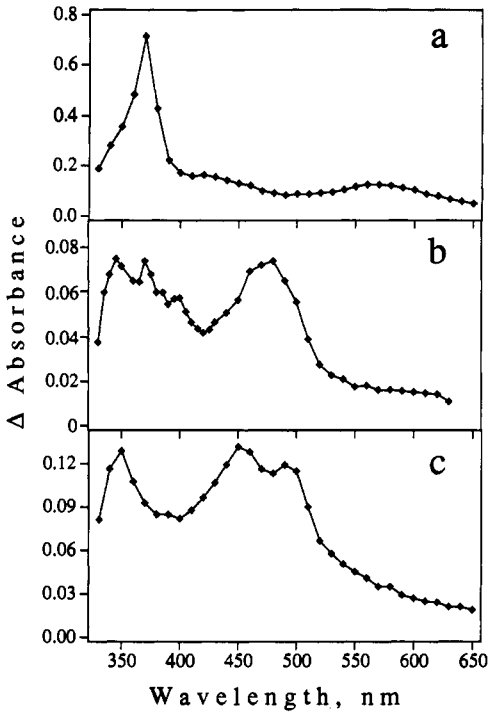

Figure 4. Transient absorption spectra obtained following 355-nm pulsed excitation from a Nd:YAG laser (6-ns fwhm, 10 mJ/pulse). All complexes were in degassed CH_3CN solution with [Re] ≈ 5 × 10^{-5} M. (a) **Re-6**, 20-ns delay; (d) **Re-5**, 0-ns delay; (c) **Re-4**, 0-ns delay.

(c) Steady-State Photochemistry of Re-1. Extensive steady-state photochemical studies were carried out on the secondary amino alcohol-substituted complex **Re-1**. All photochemistry was conducted on Ar-degassed CH_3CN solutions using 366-nm monochromatic light from either medium- or high-pressure Hg lamps. This wavelength corresponds to the MLCT absorption band of the $(bpy)Re(CO)_3^-$ chromophore.

(34) Tapolsky, G.; Duesing, R.; Meyer, T. J. *J. Phys. Chem.* **1989**, *93*, 3885.
(35) Shida, T. *Electronic Absorption of Spectra of Radical ions*; Elsevier: Amsterdam, 1988.

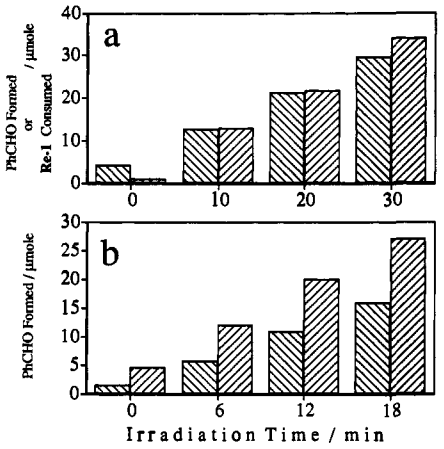

Figure 5. Rates of photochemical formation of benzaldehyde and consumption of **Re-1**. (a) Left bars, benzaldehyde formed (prompt analysis); right bars, **Re-1** consumed. (b) Left bars, benzaldehyde formed (prompt analysis); right bars, benzaldehyde formed (analysis after hydrolysis of reaction mixture for 4 days).

Several product isolation experiments were carried out to determine the overall reaction(s) which occur as a result of photolysis of **Re-1**. First, immediate postirradiation HPLC analysis indicates that benzaldehyde (PhCHO) is formed in 1:1 stoichiometry with respect to dissappearance of **Re-1** (Figure 5a). Second, semipreparative-scale photolysis of **Re-1** followed by alumina chromatography led to isolation of the major metal complex product. Spectroscopic characterization (^1H and ^{13}C NMR, high-resolution FAB mass spectrometry) indicates that the product is $[(bpy)Re(CO)_3(4\text{-}(aminomethyl)pyridine)]^+$ (**Re-8**). Third, semipreparative photolysis of a CH_3CN solution of **Re-1** followed by overnight incubation with a 5-fold excess of $NaBH_3(CN)$ (a selective reducing agent for imines)[36] led to isolation of secondary amine complex **Re-2**. Finally, since no evidence was found for the production of reduction products which are expected to accompany oxidative fragmentation of the α-AA ligand, we speculated that since reducing equivalents and protons are produced in the photoreaction, a possible ultimate reduction product could be H_2. Gas chromatography analysis of the headspace over a semipreparative-scale solution following exhaustive photolysis provided evidence that H_2 is formed in 1:1 stoichiometry with respect to dissappearance of **Re-1**.

A reaction scheme which is consistent with the experimental observations is summarized in Scheme III. Compounds which have not been isolated or whose presence has not been directly confirmed by at least two methods are shown in parentheses in this scheme. Formation of **Re-8** is envisioned to occur via a pathway that involves two-electron oxidation of **Re-1** to generate imine **Re-7** and 1 equiv of PhCHO; subsequent hydrolysis of imine **Re-7** during semipreparative chromatography produces **Re-8** and a second equivalent of PhCHO. Isolation or independent synthesis of imine **Re-7** proved impossible; however, its presence in the CH_3CN reaction mixture was indirectly confirmed by the $NaBH_3(CN)$ reduction which yielded the expected reduction product **Re-2**.

Since the stoichiometry for formation of PhCHO is important in determining the kinetic parameters (*vide infra*) further analytical experiments using HPLC were carried out to establish the time dependence of the stoichiometry for formation of PhCHO relative to dissappearance of **Re-1** (see Figure 5). These experiments indicate that "prompt" analysis (e.g., within 1-2 h of irradiation) of photoreaction mixtures gives 1:1 stoichiometry for PhCHO relative to disappearance of **Re-1** (Figure 5a); however, if the photolysis reaction mixture is allowed to stand in the dark in a 1:1 mixture of H_2O/CH_3CN for 4 days the stoichiometry approaches 2:1 for PhCHO relative to disappearance of **Re-1** (Figure 5b). Presumably the second equivalent of PhCHO is formed by slow thermal hydrolysis of the intermediate metal complex imine **Re-7**, which is formed in the primary photochemical step.

Quantum yields for the disappearance of **Re-1** (Φ^{Re}) and for prompt formation of PhCHO (Φ^{PhCHO}) were determined using the Aberchrome 540 actinometer, and the results are summarized in Table III. As can be seen from this data, Φ^{PhCHO} and Φ^{Re} are the same within experimental error (1:1 stoichiometry), and Φ^{PhCHO} is the same for $[\textbf{Re-1}]_{t=0} = 1 \times 10^{-4}$ M and $[\textbf{Re-1}]_{t=0} = 5 \times 10^{-4}$ M. The lack of a concentration dependence of Φ^{PhCHO} strongly supports the hypothesis that the photoreaction is unimolecular.

(d) Steady-State Photochemistry of Re-4. Less extensive characterization of the photoreaction was carried out for complex **Re-4**. Steady-state experiments were limited to quantitative prompt HPLC analysis of reaction mixtures to determine the amount of PhCHO produced and the amount of **Re-4** consumed by 366-nm irradiation. Quantum yield data for this reaction are summarized in Table III. Several points are of interest with respect to this data. First, it is clear that Φ^{PhCHO} and Φ^{Re} are the same within experimental error, indicating that the stoichiometry for prompt formation of PhCHO is 1:1 relative to disappearance of **Re-4**. Second, note that the overall quantum yield for photoreaction of **Re-4** is lower than for **Re-1**. This is interesting in view of the fact that MLCT quenching (formation of the LLCT state) is substantially more efficient for **Re-4**; the significance of this point will be discussed in more detail below.

Discussion

(a) Excited-State Kinetic Model. In order to relate the photophysical and photochemical results to the rate of the photochemically induced bond-fragmentation reaction which is observed for **Re-1** and **Re-4**, a kinetic and thermodynamic model must be developed (Scheme IV). Using the model presented in this scheme, the photochemical reaction is proposed to occur via the following sequence: (1) initial photoexcitation to the luminescent MLCT excited state; (2) irreversible intramolecular donor ligand-to-metal ET (with rate k_{FET}) to produce the LLCT state; and (3) irreversible C-C bond-fragmentation in the LLCT state to produce an α-amino radical (with rate k_{BF}). Note that forward ET competes with decay of the MLCT excited state via normal radiative and nonradiative pathways (with rate k_d), and bond-fragmentation competes with decay of the LLCT state via back-ET (with rate k_{BET}). Under the assumptions implied by the model presented in Scheme IV, the overall quantum efficiency for prompt formation of benzaldehyde (Φ^{PhCHO}) is given by the product of the quantum yield for formation of the LLCT state (Φ_{LLCT}) and the efficiency for bond-fragmentation within the LLCT state (β_{BF}):

$$\Phi^{PhCHO} = \Phi_{LLCT}\beta_{FB} \tag{2}$$

where

$$\Phi_{LLCT} = \left(\frac{k_{FET}}{k_{FET} + k_d}\right) \quad \text{and} \quad \beta_{BF} = \left(\frac{k_{BF}}{k_{BF} + k_{BET}}\right) \tag{3}$$

In order to more easily relate k_{BF} to experimentally accessible parameters, eqs 2 and 3 can be rearranged to express this parameter in terms of the MLCT emission lifetimes of the donor-substituted complex, the corresponding non-donor-substituted model complex (τ and τ_{model}, respectively), and the LLCT excited state (τ_{LLCT}),

(36) Lane, C. F. *Synthesis* **1975**, 135.

Scheme III

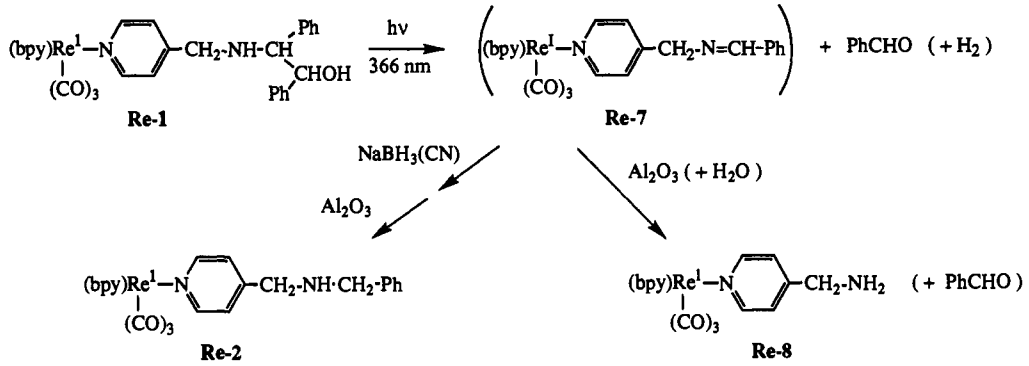

Table III. Steady-State Quantum Yields[a]

complex	[Re]/M[b]	Φ^{PhCHO} [c]	Φ^{Re} [d]
Re-1	1.0×10^{-4}	0.014 ± 0.004	0.016 ± 0.004
Re-1	5.0×10^{-4}	0.013 ± 0.002	
Re-4	5.0×10^{-4}	0.006 ± 0.001	0.007 ± 0.001

[a] All experiments in Ar-degassed CH_3CN solution with 366-nm irradiation. Values represent the average of ≥5 individual measurements; errors are standard deviations in the averages. Aberchrome 540 was used for actinometry. [b] Concentration of Re complex at $t = 0$. [c] Quantum yield for "prompt" formation of benzaldehyde. [d] Quantum yield for disappearance of starting Re complex.

$$k_{BF} = \left(\frac{\Phi^{PhCHO}}{\Phi_{LLCT}}\right)\left(\frac{1}{\tau_{LLCT}}\right) \quad (4)$$

where

$$\Phi_{LLCT} = 1 - (\tau/\tau_{model}) \quad (5)$$

The significance of eqs 4 and 5 is that k_{BF} can be determined if τ, τ_{model}, τ_{LLCT}, and Φ^{PhCHO} are known.

(b) Thermodynamics and Kinetics for Formation of the LLCT State. The kinetic model presented above indicates that the overall quantum efficiency for the photochemistry depends on both the efficiency for formation of the LLCT state, Φ_{LLCT}, and on the branching ratio for reaction within the LLCT state, β_{BF}. Because of the significance of Φ_{LLCT} in determining the overall reaction efficiency, it is important to consider how structural and thermodynamic terms influence this parameter in the two systems which have been examined in the present study.

In previous investigations it has been demonstrated that the free energy for forward ET (ΔG_{FET}) is given approximately by the following expression,[8,9]

$$\Delta G_{FET} = E_{1/2}(D/D^{\bullet+}) - E_{1/2}(bpy/bpy^{\bullet-}) - E_{0,0} \quad (6)$$

where $E_{1/2}(D/D^{\bullet+})$ and $E_{1/2}(bpy/bpy^{\bullet-})$ are electrochemical half-wave potentials for oxidation of the donor ligand and reduction of the bpy ligand, respectively, and $E_{0,0}$ is the 0–0 energy of the relaxed MLCT state which is obtained from emission spectra. Using the relevant electrochemical and spectroscopic information collected in Tables I and II, ΔG_{FET} is estimated for **Re-1** and **Re-4** (Table IV). Because the $D/D^{\bullet+}$ couples are irreversible, these ΔG_{FET} values are only approximations; however, in spite of this limitation two points are qualitatively clear: (1) ΔG_{FET} is *more* exothermic for aromatic amine-substituted complex **Re-4** than for complex **Re-1**, which features a 2° aliphatic amine donor and (2) ΔG_{FET} for **Re-1** is at best only weakly exothermic.

The rate for forward ET in a donor-substituted complex can be estimated from MLCT emission lifetimes by the following equation:[9]

$$k_{FET} = (1/\tau) - (1/\tau_{model}) \quad (7)$$

where τ and τ_{model} are emission lifetimes of the donor-substituted complex and a suitable non-donor-substituted model complex, respectively. As noted above, eq 5 allows calculation of Φ_{LLCT}, also by using the emission lifetime data. Values of k_{FET} and Φ_{LLCT} for **Re-1** and **Re-4**, calculated using the emission lifetime data and eqs 5 and 7, are collected in Table IV.

Several comments regarding the accuracy of these parameters are in order. First, for **Re-4**, it is clear that forward ET from the MLCT state is very fast; the MLCT emission decays with $k = 2 \times 10^9$ s^{-1}, which is nearly 10^3 times faster than the normal MLCT decay rate ($k_d \approx 4.8 \times 10^6$ s^{-1}). Because forward ET is so rapid in **Re-4**, $\Phi_{LLCT} = 1.0$. On the other hand, the situation regarding k_{FET} and Φ_{LLCT} for **Re-1** is somewhat less clear. Time-resolved studies indicate that τ_{em} for this complex is depressed only slightly compared to model complexes **Re-3** and **Re-6**. However, based on the fact that model complexes (e.g., **Re-3**, **Re-6**, and another model complex, (bpy)Re^{I}(CO)$_3$(4-[(*N*-benzoylamino)methyl]pyridine))[8] consistently give τ_{em} in the 210–212-ns range, we believe that the reproducible but modest suppression of τ_{em} for complex **Re-1** is due to formation of the LLCT state via forward ET. Thus, using emission lifetime data for **Re-1**, **Re-3**, and **Re-6**, it is estimated that $k_{FET} \approx 2 \times 10^5$ s^{-1} and $\Phi_{LLCT} \approx 0.05$. It is important to note that the significantly lower k_{FET} observed for **Re-1** compared to **Re-4** is in accord with the fact that ΔG_{FET} is less exothermic for **Re-1** than for **Re-4**. In addition, the absolute values of k_{FET} and their relationship to ΔG_{FET} for these two complexes are consistent with expectations based on a previous study which examined the dependence of k_{FET} on ΔG_{FET} in a series of nonreactive donor-substituted Re(I) complexes.[8]

(c) C-C Bond Fragmentation in the LLCT State: Mechanism and Estimated Rates. The primary mechanistic step which is proposed to lead to decomposition of the donor ligand is C-C bond-fragmentation in the LLCT excited state (Scheme IV). A question which is of central interest in this study concerns the rate of this bond-fragmentation reaction.

The α-AA reactive donor ligands were selected because previous bimolecular photochemical studies indicated that in α-AA$^{\bullet+}$ the σ-bond between the amine and alcohol carbon atoms undergoes heterolytic fragmentation (see eq 1) with a rate that is sufficiently fast that the process can compete with annihilation of α-AA$^{\bullet+}$ by bimolecular back-ET.[15] Although studies of this process in bimolecular systems do not allow direct measure of the rate for bond-fragmentation (k_{BF}), results suggest that in α-AAs which feature 2° or 3° amines, $k_{BF} \approx 10^5$ s^{-1}.[15a] In addition, comparison of fragmentation efficiencies for α-AAs that feature either aromatic or 3° aliphatic amines provides qualitative evidence that k_{BF} is slower in the aromatic α-AA systems.[15a]

As noted above, under the assumption that the mechanism in Scheme IV is correct, k_{BF} can be calculated for **Re-1** and **Re-4** from the values of Φ^{PhCHO}, Φ_{LLCT}, and τ_{LLCT} by using eq 4. All of these parameters are available for **Re-4**: Φ^{PhCHO} and Φ_{LLCT} were obtained from steady-state photochemical measurements and emission studies, respectively, and τ_{LLCT} was obtained by

Scheme IV

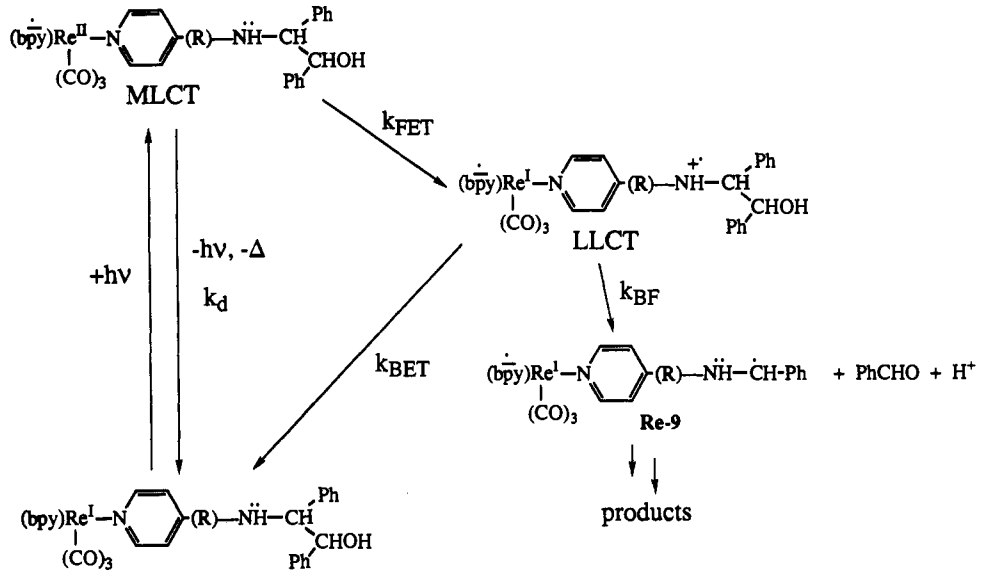

Table IV. Estimated ET Free Energies, ET Rates, and Bond Fragmentation Rates[a]

complex	ΔG_{FET}/eV	ΔG_{BET}/eV	k_{FET}/s^{-1}	Φ_{LLCT}	k_{BET}/s^{-1}	k_{BF}/s^{-1}
Re-1	0 ± 0.2	−2.4 ± 0.2	2.2×10^5	0.05	$\approx 1 \times 10^7$	$\approx 4 \times 10^6$
Re-4	−0.27	−2.11	2.0×10^9	1.0	8.3×10^7	5.0×10^5

[a] CH_3CN solution, 25 °C.

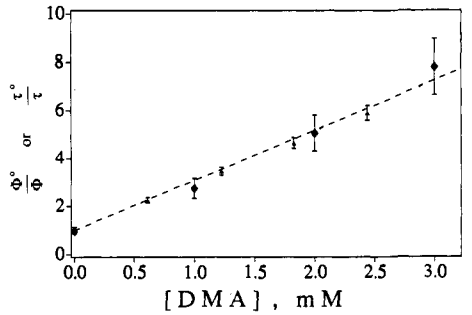

Figure 6. Stern–Volmer quenching of **Re-1** MLCT emission lifetime (τ) and quantum yield for benzaldehyde formation (Φ) by DMA. (▲) emission lifetime quenching (τ°/τ); (♦) quantum yield quenching (Φ°/Φ).

laser flash photolysis. Using these data for **Re-4** we estimate $k_{BF} = 5 \times 10^5\ s^{-1}$.

By contrast, the kinetics are less well-defined for complex **Re-1**. Although Φ^{PhCHO} and Φ_{LLCT} are available for this complex, direct measurement of τ_{LLCT} by laser flash photolysis was not possible. Detection of the LLCT state in **Re-1** by flash photolysis is precluded because (1) Φ_{LLCT} is small and (2) the 2° aliphatic amine radical cation does not absorb strongly in the near-UV or visible region.[35] Thus, in an effort to provide an estimate for τ_{LLCT} for **Re-1**, a Stern–Volmer (S-V) experiment was carried out in which *N,N*-dimethylaniline (DMA) was used to quench the bond-fragmentation reaction by reductive ET from DMA to the LLCT state, $(bpy^{\bullet-})Re^{I}(CO)_3(D\text{-}R^{\bullet+})$. Because DMA also quenches the MLCT state, a parallel experiment was conducted to determine the efficiency of S-V quenching of the MLCT emission by DMA. The result of this experiment is presented in Figure 6, where ($\Phi^{\circ\ PhCHO}/\Phi^{PhCHO}$) and ($\tau_{em}^\circ/\tau_{em}$) are plotted vs [DMA]. This experiment indicates that, as expected, DMA quenches the MLCT state at the diffusion-controlled rate ($k_q^{MLCT} = 1.1 \times 10^{10}\ M^{-1}\ s^{-1}$). However, S-V quenching of Φ^{PhCHO} exactly parallels quenching of the MLCT emission. The parallel quenching of τ_{em} (MLCT) and Φ^{PhCHO} indicates two important features: (1) quenching of the LLCT state, if it occurs at all, is too inefficient to detect and (2) the MLCT state is clearly a precursor in the mechanism leading to bond-fragmentation, consistent with the proposed mechanism in Scheme IV.

Two possible reasons can be suggested to explain the lack of LLCT quenching in the S-V experiment. The first is that the bimolecular rate constant for interception of the LLCT state by DMA is large (e.g., $k_q^{LLCT} \geq 10^9\ M^{-1}\ s^{-1}$), but τ_{LLCT} is short (e.g., $\tau_{LLCT} \leq 100$ ns), so that the overall quenching efficiency is low. The second is that bimolecular quenching is slow (e.g., $k_q^{LLCT} \ll 10^9\ M^{-1}\ s^{-1}$), and therefore, regardless of how long-lived the LLCT state is, the quenching efficiency is low. We favor the former explanation for two reasons. First, electron transfer from DMA to the LLCT state should be relatively fast: studies of self-exchange ET between amines and their radical cations indicate that the reorganization energy for ET is low, and the reaction between DMA and the LLCT state is exothermic by ≥0.3 eV.[37] Second, studies of the decay of the LLCT state in nonreactive donor-substituted Re(I) complexes lead to the prediction that for **Re-1**, $\tau_{LLCT} \approx 100$ ns.[8] Thus, with these caveats in mind, we have used $\tau_{LLCT} = 100$ ns to provide an estimate for k_{BF} in **Re-1** of $4 \times 10^6\ s^{-1}$.[38]

An interesting feature now emerges upon comparison of k_{BF} for complexes **Re-1** and **Re-4**: bond-fragmentation is apparently much faster in the 2° aliphatic amine donor ligand (**Re-1**) than in the 2° aromatic amine donor ligand (**Re-4**). This disparity in k_{BF} values provides a rationale for the observation that Φ^{PhCHO} is comparable in the two systems, despite the fact that Φ_{LLCT} is significantly larger for **Re-4** compared to **Re-1**. Apparently the high efficiency of Φ_{LLCT} in complex **Re-4** is offset by a comparatively lower k_{BF}. Note that the finding that k_{BF} is greater for the aliphatic α-$AA^{\bullet+}$ is consistent with the qualitative results based on bond-fragmentation efficiencies in bimolecular systems.[15a]

An important question concerns the origin of the disparity in k_{BF} values for the two reactive donor ligands. It is clear that there is an interaction between the electrophilic N-centered radical cation and the C-C σ-bond (σ_{CC}) which weakens the C-C bond. This interaction can be viewed as hyperconjugation between the half-filled N p orbital and the filled σ_{CC} orbital (Chart I). The hyperconjugation reduces the bond order of σ_{CC}, and therefore the bond is susceptible to relatively rapid heterolytic fragmentation

(37) (a) Grammp, G.; Jaenicke, W. *Ber. Bunsen Ges. Phys. Chem.* **1984**, *88*, 325. (b) Grammp, G.; Jaenicke, W. *Ber. Bunsen Ges. Phys. Chem.* **1984**, *88*, 335. (c) Grammp, G.; Jaenicke, W. *J. Chem. Soc., Faraday Trans. 2* **1985**, *81*, 1035.

(38) If $\tau_{LLCT} < 100$ ns, then the value of k_{BF} calculated using eq 4 would be $> 4 \times 10^6\ s^{-1}$, and therefore the conclusion that k_{BF}(**Re-1**) > k_{BF}(**Re-4**) would still be valid.

Chart I

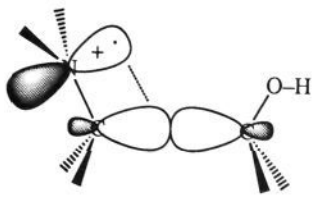

at ambient temperatures. Importantly, as the electrophilicity of the N-centered radical cation center increases, interaction between the N p orbital and the σ_{CC} orbital increases and the σ_{CC} bond order decreases. The influence of the aryl group on the reactivity of α-AA$^{\bullet+}$ can be explained within this model because it will effectively decrease the electrophilicity of the N-centered radical by delocalizing the spin-density into the aryl ring. This delocalization effectively decreases the hyperconjugative interaction and increases the bond order of σ_{CC}.

(d) Dark Reactions of the Re α-Amino Radical: Concerning the Mechanism for Ultimate Product Formation. To this point the discussion has centered on the mechanism leading to C-C bond-fragmentation in the LLCT state. The photophysical and photochemical results are consistent and indicate that the primary photophysical sequence shown in Scheme IV culminates in formation of reactive intermediate **Re-9**, which is a Re(I) complex that contains a bpy anion radical ligand and an α-amino radical ligand. While no direct experimental information is available concerning the reactivity of **Re-9**, it is of some interest to speculate on the pathway which is followed during decomposition of this reactive intermediate.

First, it is important to note that α-amino radicals are highly reducing; transient electrochemical experiments indicate that the half-wave potential for the α-amino radical/iminium ion couple (e.g., $E_{1/2}^{ox}(R_2N{-}\dot{C}HR/R_2N^{+}{=}CHR)$) is in the range –0.9 to –1.2 V vs SCE.[39] Consistent with the highly reducing nature of the α-amino radical is the fact that the following decay pathway *does not* operate for reactive intermediate **Re-9**: This reaction

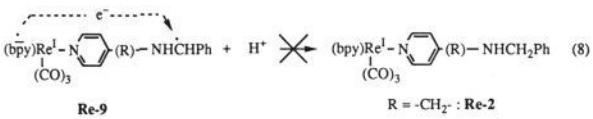

would involve intramolecular ET *from* the bpy anion radical *to* the α-amino radical site. Protonation of the resultant carbanion would form **Re-2**; however, **Re-2** is not observed in the product mixture following photolysis of **Re-1**.

Because the product studies strongly suggest that the final photoproduct of **Re-1** is imine **Re-7**, which results from two-electron oxidation of the α-AA ligand, considerable effort was expended to determine the ultimate fate of the reducing equivalents generated during the reaction. Since (bpy)Re^{I}(CO)$_3$L complexes undergo one-electron reduction of the coordinated bipyridine ligand at relatively low cathodic potentials (Table I) and the one-electron reduction products (bpy$^{\bullet-}$)Re^{I}(CO)$_3$L are typically stable in the absence of O_2, we felt that it was possible that the reducing equivalents could accumulate in the form of one-electron-reduced starting Re complex. The reduced metal complex (bpy$^{\bullet-}$)Re^{I}(CO)$_3$L has a strong absorption band at ≈370 nm due to the coordinated bpy anion radical.[40] Therefore, if metal complex reduction occurs during photoreaction under an inert atmosphere, it should be possible to detect the buildup of bpy$^{\bullet-}$ by UV absorption spectroscopy. However, repeated experiments on samples contained in dry and degassed CH_3CN provided no evidence for the appearance of the UV absorption characteristic of metal complex reduction.

Due to the lack of evidence for the accumulation of (bpy$^{\bullet-}$)Re^{I}(CO)$_3$L, or for that matter any other reduction products, we reasoned that the only alternative was that H^+ might be reduced to H_2 (H^+ should be produced during the C-C bond fragmentation process, see Scheme IV). In order to test this hypothesis, a gas chromatographic analysis was carried out on a 10-mg sample of **Re-1** contained in 3 mL of CH_3CN which had been subjected to exhaustive photolysis. This experiment provided evidence that H_2 gas is formed in approximately the stoichiometry expected from the following equation (the required equivalent of H^+ is generated in the C-C bond fragmentation reaction):

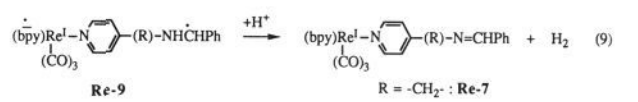

Note that eq 9 describes an overall reaction; insufficient experimental information is available at the present time to allow any conclusions to be drawn concerning the mechanism or the species that might catalyze the $2e^-$, $2H^+$ reduction reaction. However, note that (dimine)Re(CO)$_3$L complexes catalyze the reduction of CO_2 to HCO_2H, a process in which the Re complex catalyzes a $2e^-$ reduction.

Conclusion

This study has examined the efficacy of using reactive donor ligands to probe the electronic structure and dynamics of the LLCT state in (bpy)Re(CO)$_3$L complexes. The results indicate that the concept works; however, this project defines some limitations which must be overcome if the method is to become generally useful. The most prominent limitation is that the reaction which is triggered by donor-ligand oxidation must be sufficiently fast that it competes effectively with decay of the LLCT state by back-ET. The α-AA-based reactive donor ligands fragment comparatively slowly relative to the rate for back-ET and, as a result, the overall quantum efficiency for photochemistry in these systems is low. One goal of future studies will be to explore reactive donor systems which undergo faster reactions upon single ET activation.

An interesting finding of the present study is the significantly different fragmentation rates for the radical cations of the 2° aliphatic and the 2° aromatic amino alcohols. The difference in reactivity is qualitatively rationalized by considering factors which stabilize the amine radical cations; however, further studies are clearly warranted to carefully explore the relationship between the thermodynamic stability of the radical cations and the rate for C-C bond-fragmentation.[42]

Acknowledgment. This work was supported by a grant from the National Science Foundation (CHE-9123000). Acknowledgement is made to the donors of the Petroleum Research Fund, administered by the American Chemical Society, for partial support of this work in the form of an Undergraduate Summer Research Fellowship for M. M. Rooney.

(39) Hawari, J. A.; Kanabus-Kaminska, J. M.; Wayner, D. D. M.; Griller, D. In *Substituent Effects in Radical Chemistry*; Viehe, H. G., Janousek, Z., Merenyi, R.; Eds.; D Reidel: Boston, 1986.

(40) MacQueen, D. B.; Schanze, K. S., unpublished.

(41) (a) O'Toole, T. R.; Margerum, L. D.; Westmoreland, T. D.; Vining, W. J.; Murray, R. W.; Meyer, T. J. *J. Chem. Soc., Chem. Commun.* **1985**, 1416. (b) Sullivan, B. P.; Bolinger, C. M.; Conrad, D.; Vining, W. J.; Meyer, T. J. *J. Chem. Soc., Chem. Commun.* **1985**, 1414.

(42) Venimadhavan, S.; Amarnath, K.; Harvey, N. G.; Cheng, J.-P.; Arnett, E. M. *J. Am. Chem. Soc.* **1992**, *114*, 221.